LCLS-TN-99-1
SLAC-AP-117
March 1999

The Resonator Impedance Model of Surface Roughness Applied to the LCLS Parameters*

Karl L.F. Bane
Stanford Linear Accelerator Center, Stanford University, Stanford, CA 94309
Alexander Novokhatskii
Technische Universität Darmstadt, Darmstadt, Germany

Abstract

The resonator impedance model of surface roughness in a cylindrical beam tube, derived in Ref. 1, is compared to the inductive impedance model of Ref. 2. It is shown that for long, smooth bunches the two models both give an inductive response, that the effective inductance per length is proportional to the corrugation depth over the beam pipe radius, and that the absolute results also are comparable. For a non-smooth bunch shape, such as is found in the undulator region of the LCLS, however, the inductive impedance model is no longer valid; and the resonator model gives a non-inductive response, with the induced energy spread decreasing much more slowly with increasing bunch length than for a smooth distribution. When applied to the actual bunch shape and parameters in the LCLS, the resonator model predicts that, to remain within tolerances for induced energy spread, the beam tube roughness must be kept to ~ 10 nm. Further calculations suggest, however, that if the period-to-depth aspect ratio of the surface features is large, (as has been found in recent measurements of polished beam tube surfaces), then the wakefield effect may be greatly suppressed, and the roughness tolerance greatly increased.

*Work supported by Department of Energy contract DE–AC03–76SF00515.

[1] A. Mosnier and A. Novokhatski, Proceedings of 1997 Part. Accel. Conf., Vancouver, Canada, p. 1661.

[2] K.L.F. Bane, C.K. Ng and A.W. Chao, Proceedings of 1997 Part. Accel. Conf., Vancouver, Canada, p. 1738, SLAC-PUB-7514 (1997).

The Resonator Impedance Model of Surface Roughness Applied to the LCLS Parameters

Karl L.F. Bane, Stanford Linear Accelerator Center, Stanford, USA
Alexander Novokhatski, Technische Universität Darmstadt, Germany

Abstract

The resonator impedance model of surface roughness in a cylindrical beam tube, derived in Ref. [1], is compared to the inductive impedance model of Ref. [2]. It is shown that for long, smooth bunches the two models both give an inductive response, that the effective inductance per length is proportional to the corrugation depth over the beam pipe radius, and that the absolute results also are comparable. For a non-smooth bunch shape, such as is found in the undulator region of the LCLS, however, the inductive impedance model is no longer valid; and the resonator model gives a non-inductive response, with the induced energy spread decreasing much more slowly with increasing bunch length than for a smooth distribution. When applied to the actual bunch shape and parameters in the LCLS, the resonator model predicts that, to remain within tolerances for induced energy spread, the beam tube roughness must be kept to $\sim$ 10 nm. Further calculations suggest, however, that if the period-to-depth aspect ratio of the surface features is large, (as has been found in recent measurements of polished beam tube surfaces), then the wakefield effect may be greatly suppressed, and the roughness tolerance greatly increased.

Introduction

In many future accelerators the peak current is high, the bunch length is very short, and the nominal energy spread and emittance are small. For example, in parts of the linac and in the undulator region of the Linear Coherent Light Source (LCLS) the peak current is 3.4 kA, the rms bunch length is 20 μm, the rms energy spread is 0.1%, and the normalized emittance is 1 mm-mr[3]. One concern in such machines is that induced wakefields may significantly increase the beam energy spread or the emittance, and may interfere with lasing. It has been pointed out in [1, 2] that one major source of wakefields in machines with very short bunches might be the roughness of the inner

beam pipe surface. In the LCLS this is most serious in the undulator region where, in order not to interfere with lasing, the change in energy deviation must be kept to within $\pm 0.1\%$[4].

One approach to estimating the roughness impedance uses a model that we here will call the "inductive impedance model"[2]. This model was derived by considering a rough surface as a collection of simple bumps on a smooth surface, with the total impedance approximated by the sum of impedances of the individual bumps. If the bump dimensions are small compared to the bunch length, then the impedance of a bump will be nearly purely inductive, and, according to this model, the impedance of the entire rough surface will also be nearly purely inductive. The longitudinal impedance of a cylindrical tube with a rough surface is given by

$$Z(\omega) = -i\omega\mathcal{L} = -i\omega\alpha f \frac{Z_0 \Delta L}{2\pi c a} \quad , \tag{1}$$

with ω the frequency, $\mathcal{L}$ the effective inductance, α a packing factor equal to the fraction of the surface occupied by bumps, f a form factor depending on the typical shape of a bump, $Z_0 = 120\pi\Omega$, Δ the size of a typical bump (more precisely, it is defined such that the surface area of the base of the bump equals $\pi\Delta^2$), L the tube length, c the speed of light, and a the beam tube radius. The inductance per unit length is thus given by

$$\frac{\mathcal{L}}{L} = \alpha f \frac{Z_0 \Delta}{2\pi c a} \quad . \tag{2}$$

Form factors f for various shapes of bumps were obtained numerically. It was found that f equals 1 for a hemisphere, and varies over $0.5 \lesssim f \lesssim 2.5$ for similar objects, such as a half-cube, etc. When changing shape the strongest sensitivity of f is on bump height, with nearly a quadratic dependence. Note that an inductive result for the impedance of a rough surface has also been obtained using an analytical, perturbative approach, one that can, in addition, account for the interaction between various bumps[5]. In the specific case of a surface with non-interacting, smooth bumps it can be shown that these inductive models give the same result[6].

A completely different impedance model, one that we will call the "resonator impedance model," was presented in Ref. [1]. The authors began by representing a rough surface by a tube with periodic, shallow corrugations. Through time-domain simulations they find that the resulting wakefield is well approximated by a single, loss-free resonator wakefield. The authors note that the same kind of impedance is found for a beam tube with a thin dielectric layer[7],[8]. An important (and maybe surprising) result in Ref. [1]

is that when the surface with the periodic perturbations is replaced by one with random perturbations, the character of the wakefield experienced by the beam is left unchanged, and the resonator model still is valid. Note that M. Dohlus[9], beginning with the the general properties of a surface impedance, has obtained a result that is in very close agreement with this model.

In the LCLS design report the inductive impedance model was used to estimate the wakefield effect of surface roughness. The goal of the present report is to study the connection between the inductive and the resonator models, and to apply the latter to the LCLS parameters. In this regard we will focus on the longitudinal effect in the undulator region, since that seems to be where the critical problem resides. Note, however, that once the longitudinal effect is known, the transverse effect can be easily obtained (see, *e.g.* Ref. [2]). We begin this report by describing the resonator impedance model. We then further explore the impedance of a tube with shallow, periodic corrugations, this time using a frequency domain approach. Next we discuss the wakefield of a bunch in the presence of the resonator impedance, the results of which we then apply to the LCLS parameters. Then we briefly discuss an experiment that can be performed in the SLAC linac to measure the strength of a roughness impedance. In Appendix A we present a derivation of impedance properties of a pipe with shallow, periodic corrugations. Finally, in Appendix B, we investigate the dependence of the impedance of the periodic model on the period-to-depth ratio of the wall perturbations.

The Resonator Impedance Model[1][10]

Let us consider a cylindrical, metallic beam pipe which has small perturbations on its interior surface. (In this report we assume that the perturbations are large compared to the skin depth of the pipe material, and that we can ignore the wall resistivity. For a roughness study that does not make this assumption, see Ref. [11].) According to Refs. [1], [10] the interaction of a bunch with such a beam pipe is similar to the interaction with a beam pipe with shallow, *periodic* corrugations, or that of a metallic beam tube with a thin dielectric coating. In either case the wakefield is given by that of a single, loss-free resonator. In the dielectric case, it is written as:

$$W_z(s) \approx \frac{Z_0 c}{\pi a^2} \cos ks \qquad , \qquad s > 0 \quad , \tag{3}$$

with wave number

$$k = \sqrt{\frac{2\epsilon}{(\epsilon - 1) a \delta'}} \qquad ; \tag{4}$$

ϵ is the dielectric constant, a the tube radius, and δ' the depth of the dielectric layer. The transverse wakefield is a resonator wakefield of the same frequency

$$W_x(s) \approx \frac{2Z_0 c}{\pi a^4 k} \sin ks \qquad , \qquad s > 0 \quad . \tag{5}$$

From two-dimensional, time-domain simulations of a corrugated pipe with depth and period approximately equal this model appears to agree if δ' is taken to equal the typical depth of corrugation and ϵ is taken to be about 2. From three-dimensional simulations of a cylindrical pipe with random perturbations on the surface it was observed that the resonator model still seems to be valid, but with the effective depth δ' now taken to be about a factor of 3 smaller than the actual typical perturbation size. Therefore, the wave number becomes

$$k_{3d} = \sqrt{\frac{12}{a\delta}} \qquad , \tag{6}$$

with δ the size of the typical perturbation.

Note that, in reality, there are many modes in a corrugated pipe, or in a tube with a thin dielectric layer, and Eqs. 3 and 5 represent only the contribution of the lowest, dominant mode. The contribution of the higher modes, however, is extremely small, and can be ignored. This is reflected in the fact that the amplitudes in Eqs. 3 and 5 are taken to be equal to the (theoretical) sum of the amplitudes of all the modes in a periodic structure[12, 13].

Transient Behavior

The above results are meant to represent the asymptotic, steady-state wake functions. When a bunch, whose length is long compared to the size of the wall perturbations, first enters into the beam tube the wakefield interaction will be almost purely inductive, *i.e.* the shape of the bunch wakefield will be proportional to the derivative of the bunch shape, and the losses will be almost zero. Eventually, however, a significant resistive component may develop. As an illustration of such a progression we present in Fig. 1 results of a numerical time domain calculation[14]. The bunch shape is Gaussian with an rms length $\sigma = 50$ μm, and the rough surface is represented by a periodically corrugated tube, with tube radius $a = 5$ mm, a depth of corrugation of 10 μm, a period of 20 μm, and a gap of 10 μm. Shown is the wakefield per cell after 1, 10, 1000, 10000, 20000, and 30000 periods. We see that the bunch needs to pass about 20000 periods, or 40 cm of this structure, for the wakefield to begin to reach steady-state. As an estimate

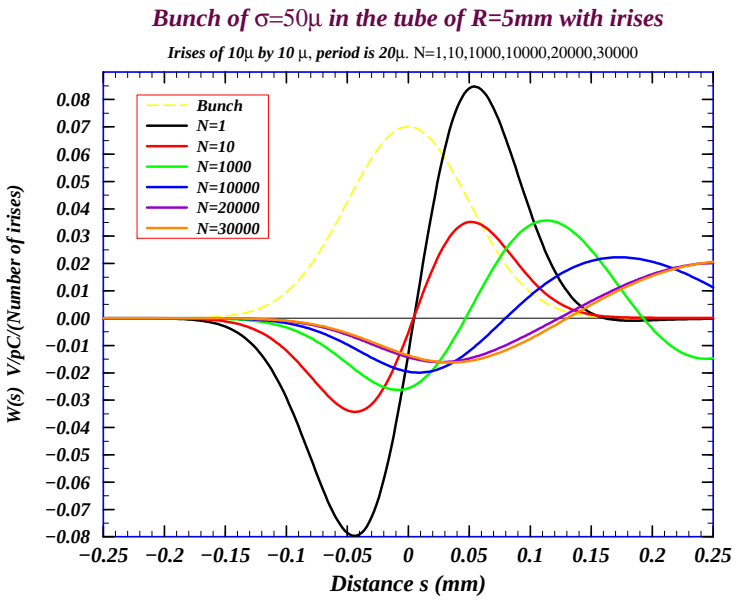

Figure 1: Results of time domain calculations of a model of a rough surface showing transient effects. The bunch is Gaussian with an rms length of 50 μm. The structure is a tube with periodic corrugations, with $a = 5$ mm, a depth of corrugation of 10 μm, a period of 20 μm, and a gap of 10 μm. The bunch wake per cell is given after 1, 10, 1000, 10000, 20000, and 30000 periods.

of the distance to steady-state, if we use a formula derived for accelerating structures[15]

$$z_{crit} = \frac{a^2}{2\sigma} \quad , \tag{7}$$

we find that $z_{crit} = 25$ cm, which is in reasonable agreement with the numerical results. Note, however, that in the LCLS undulator $a = 2.5$ mm and the rms bunch length $\sigma = 20$ μm; therefore, $z_{crit} = 16$ cm, which is negligible compared to the length of the undulator, 112 m. Thus, in the following we will ignore the transient effect.

The Impedance of a Tube with Shallow, Periodic Corrugations

Since the impedance of a cylindrical pipe with shallow, random wall perturbations appears to be closely related to that of a cylindrical pipe with shallow, periodic perturbations, we begin by studying the latter case in more

detail. Such a study was performed in Ref. [1] using a time domain computer program; our study here will use a frequency domain approach. The geometry that we consider is sketched in Fig. 2, showing the beam tube radius a, the depth of corrugation δ, the gap g, and the period p. By "shallow" we mean to indicate that $\delta/a \ll 1$, but for now we assume that $p/\delta \lesssim 1$. It is not generally appreciated that for such a situation there is usually one dominant mode with a frequency as low as $k \sim 1/\sqrt{a\delta}$. Many years ago Chatard-Moulin and Papiernik applied a perturbation approach to obtaining the monopole ($m = 0$) modes in such a structure[16]. (The approach was later repeated by Cooper, *et al*, for the dipole ($m = 1$) modes[17].) This method finds no mode with $k \sim 1/\sqrt{a\delta}$; instead it finds a collection of narrowly spaced, very weak modes, all at much higher frequencies, $kp \gtrsim \pi$. Note, however, that for this approach to be valid, requires that both the depth of perturbation (δ/a) and the slope of the wall perturbation be everywhere small; it is, therefore, not applicable to the geometry of our problem.

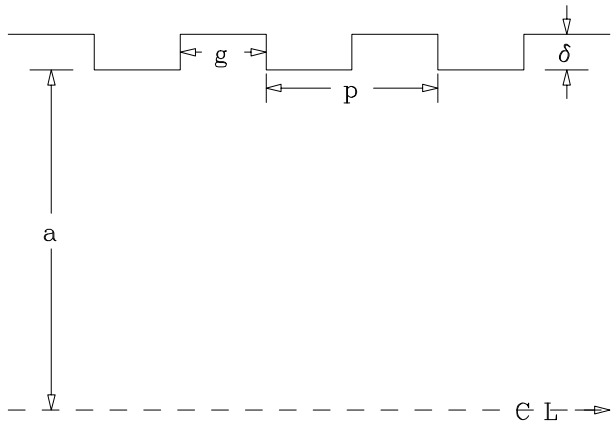

Figure 2: The geometry used in the simulations.

To investigate the impedance of our corrugated model we use the field matching program TRANSVRS[18]. First, if we take the formalism of this program, truncate the (infinite dimensional) system matrix to dimension 1, we obtain the synchronous frequency of the lowest mode (see Appendix A):

$$k_0 = \sqrt{\frac{2p}{a\delta g}} \quad , \tag{8}$$

and its loss factor

$$\varkappa_0 = \frac{Z_0 c}{2\pi a^2} \quad . \tag{9}$$

These equations are valid so long as δ/a is small, and p/δ is not large. Note that for $p/g = 2$ these results are the same as that of the dielectric layer model (Eq. 4) with $\epsilon = 2$. As a numerical example let us consider the parameters $\delta/a = 0.025$, $p/a = 0.050$ and $g/a = 0.025$; for the calculations we include 20 harmonics in the cavity region, and 40 in the beam tube region. We obtain from TRANSVRS the $(m = 0)$ dispersion curve shown in Fig. 3, with the synchronous point indicated by the plotting symbol. Note that at the synchronous point the group velocity v_g is very nearly the speed of light. An estimate,

$$(1 - v_g/c) = \frac{4\delta g}{ap} \qquad , \tag{10}$$

is derived in Appendix A. Note also that the next higher synchronous modes are just beyond π phase advance, *i.e.* at $kp \gtrsim \pi$, are very closely spaced, and are very weak. For this example their loss factors are down by 3 orders of magnitude. Note also that for the much smaller undulation size appropriate for the LCLS beam pipe (with $a = 2.5$ mm, if $\delta \sim 1\ \mu$m, then $\delta/a \sim 4\times10^{-4}$), the position of the first synchronous mode moves very close to zero phase advance, and the magnitudes of the next higher modes reduce even further.

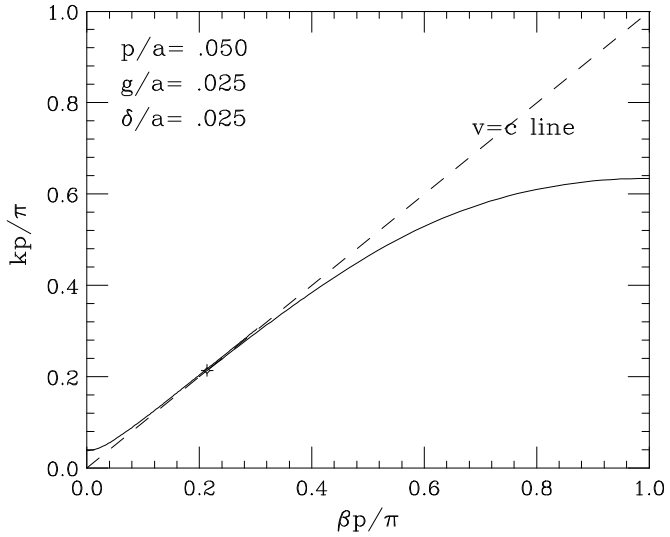

Figure 3: Dispersion curve for a beam tube with small, periodic undulations.

We have performed more numerical calculations to study the p/g dependence of the resonant frequency (still for the case p/δ not large). See Fig. 4. Shown are the numerically calculated first two mode frequencies (the plotting symbols), the analytical formula Eq. 8, and the formula $kp = \pi$. We

note that the first two modes are well approximated by these formulas, and that as the period increases the frequency of the first mode approaches that of the next higher mode. For the transverse (dipole) case, again taking the field-matching formalism of TRANSVRS and truncating the system matrix to dimension 1, we find that the frequency dependence is again approximately given by Eq. 8. The observation that the dipole mode frequency is the same as the longitudinal frequency was also found in Ref. [10].

Although we are interested here in the microscopic features of the beam pipe surface, the results of this section do not require such extremely small features in order to be applicable. For example, in Ref. [19] numerical results are given for the case of unshielded bellows for a storage ring, with $\delta/a = 0.2$ and $p/a = 0.13$, results which agree quite well with those presented here.

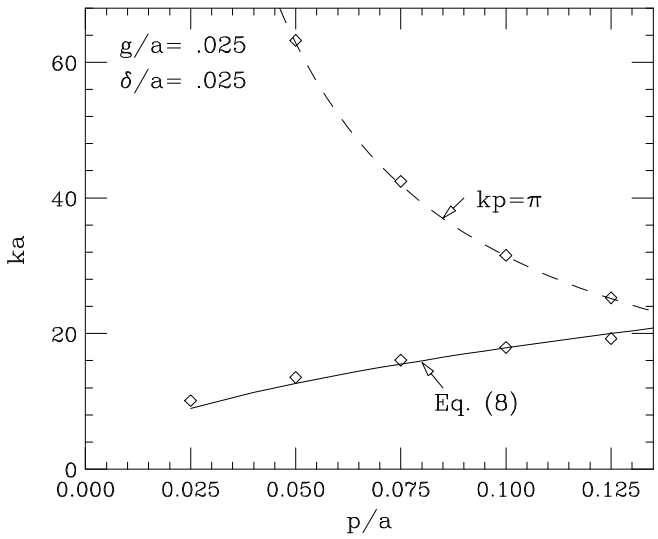

Figure 4: Dependence of resonance frequency k on period p for the first two synchronous modes, when the depth δ and gap g are kept fixed (the plotting symbols).

The Energy Deviation Induced within a Bunch

In an FEL there is a tolerance on the increase in energy deviation of particles within a bunch during the passage through the undulator. The main source of such an increase likely is the roughness wakefield of the undulator beam pipe. The voltage induced by a bunch in a tube of length L due to wakefields is given by $V_{ind} = eNL\bar{W}_z$, with eN the bunch charge and $\bar{W}_z$ the bunch

(longitudinal) wake, given by

$$\bar{W}_z(s) = -\int_0^\infty \lambda(s-s')W_z(s')\,ds' \qquad , \tag{11}$$

with λ the longitudinal bunch distribution (and similarly in the transverse case). We convert a bunch wake to relative energy deviation:

$$\delta_E = \frac{e^2 N \bar{W}_z L}{E} \qquad , \tag{12}$$

with E the beam energy. Two quantities, useful in characterizing the bunch wake are the total loss per unit charge (also called the bunch loss factor)

$$\bar{\varkappa} = -\langle \bar{W}_z \rangle = -\int_{-\infty}^\infty \lambda(s)\bar{W}_z(s)\,ds \qquad , \tag{13}$$

and the rms value $(\bar{W}_z)_{rms}$. In energy, the corresponding parameters are the average energy loss $\langle \delta_E \rangle$ and the rms energy deviation $(\delta_E)_{rms}$.

A Smooth Bunch Shape

Suppose that the resonator frequency is much higher than the frequencies within the bunch spectrum. In such a case we expect the wakefield interaction to be inductive in character; *i.e.* the bunch wake will be approximately proportional to the derivative of the bunch distribution. The induced voltage can then be written as $V_{ind} = -eNc\mathcal{L}\lambda'$, with $\mathcal{L}$ the inductance, a constant. For the resonator wake Eq. 11 becomes

$$\bar{W}_z(s) = -2\varkappa_0 \int_0^\infty \lambda(s-s')\cos ks'\,ds' \qquad , \tag{14}$$

with $\varkappa_0$ the mode loss factor. If the frequency spectrum of the bunch is confined to frequencies much lower than k, then we obtain the inductive bunch wake

$$\bar{W}_z(s) \approx -\frac{2\pi\varkappa_0}{k^2}\lambda'(s) \qquad , \tag{15}$$

with the effective inductance per length

$$\frac{\mathcal{L}}{L} = \frac{2\pi\varkappa_0}{k^2 c} \qquad . \tag{16}$$

How does this result compare with the inductance obtained by the inductive impedance model, Eq. 2? If we substitute Eq. 6 into Eq. 16, we

see that both inductances are proportional to the ratio of the depth of the perturbation to the beam tube radius. To get an idea of the relative size of the constants, let the surface packing factor $\alpha = 0.5$ in the inductive model correspond to $p/g = 2$ in the resonator model and Δ correspond to $\delta/2$. Then we find that the two models give equal results if in the inductive model the form factor $f = 2.$, which is approximately what we expect (for the half cube shape, $f = 2.6$). Thus, although the two models are quite different, for the case when the bunch is long compared to the perturbation size, and smooth, they give quite comparable results.

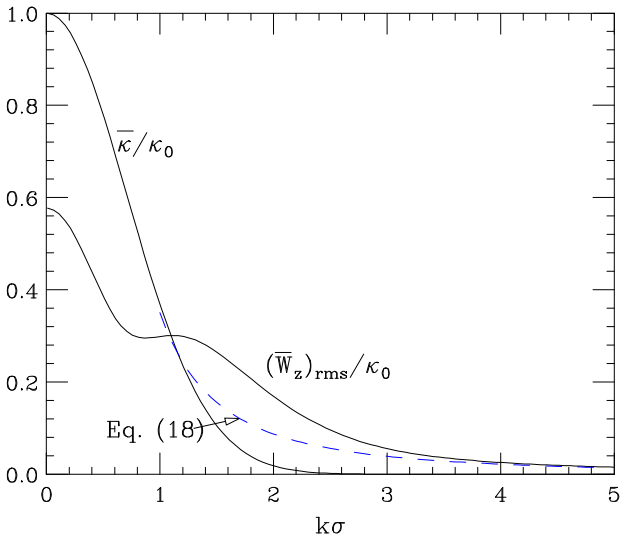

Figure 5: The interaction of a Gaussian bunch of length σ and the resonator wakefield with amplitude $2\varkappa_0$ and frequency k. Shown are the total bunch loss $\bar{\varkappa}$ and $(\bar{W}_z)_{rms}$ (the solid lines) and the asymptote, Eq. 18 (the dashes).

Consider now the specific case of a Gaussian bunch distribution, with σ the rms bunch length, in the presence of the resonator impedance. From Eqs. 13,14 we find that the bunch loss factor is given by

$$\bar{\varkappa} = \varkappa_0 e^{-k^2\sigma^2} \qquad . \tag{17}$$

For $k\sigma \gtrsim 2$ this parameter becomes very small. In Fig. 5 we plot this result and also the numerically obtained $(W_z)_{rms}$ for a Gaussian bunch. For $k\sigma \gtrsim 4$ it is approximately given by

$$(\bar{W}_z)_{rms} = \frac{2^{1/2}}{3^{3/4}\pi^{1/2}} \frac{\varkappa_0}{k^2\sigma^2} \qquad , \ [k\sigma \text{ large}]. \tag{18}$$

The parameter $(\bar{W}_z)_{rms}$ decreases as $(k\sigma)^{-2}$ for large $k\sigma$. Note that, in comparison, the inductive impedance model gives $\bar{\varkappa} = 0$ and $(\bar{W}_z)_{rms} = c^2/(2^{1/2}3^{3/4}\pi^{3/2}\sigma^2) \times(\mathcal{L}/L)$. Finally, in Fig. 6 we display the bunch wake for a short ($k\sigma = 2$) and long ($k\sigma = 8$) Gaussian bunch in the presence of a resonator impedance. Note that in the long bunch case the bunch wake is very nearly proportional to the derivative of the (Gaussian) bunch distribution; *i.e.* the response is inductive.

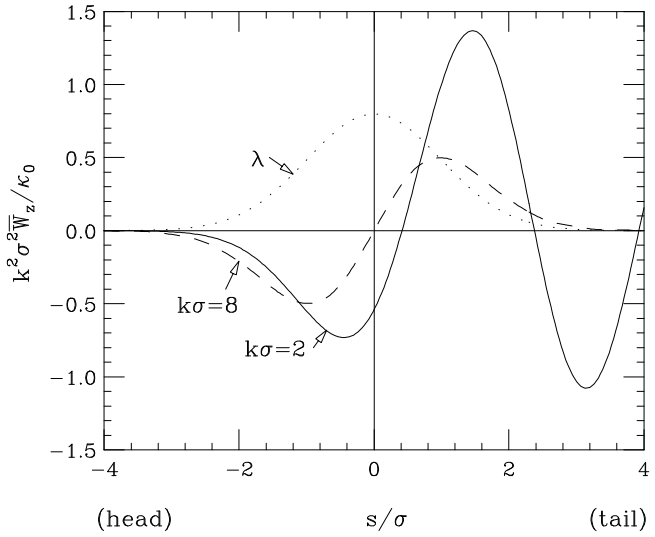

Figure 6: The bunch wake for a Gaussian bunch in the presence of a resonator wakefield, when $k\sigma = 2$ and $k\sigma = 8$.

A Non-Smooth Bunch Shape

The expected bunch shape in the LCLS undulator is rather rectangular in shape. This result is due to the two upstream bunch compressions, and due to the shape of the longitudinal wakefield in the linac, and is something that cannot easily be changed[20]. If the bunch is not smooth, *i.e.* if there are high frequency components in the spectrum, then the correspondence in the two roughness impedance models found for long bunches is no longer true. In fact, for such a case the inductive model is not valid.

For a rectangular distribution, with full-width $\Delta = 2\sqrt{3}\sigma$, in the presence of a resonator impedance we find that the bunch wake (over the bunch)

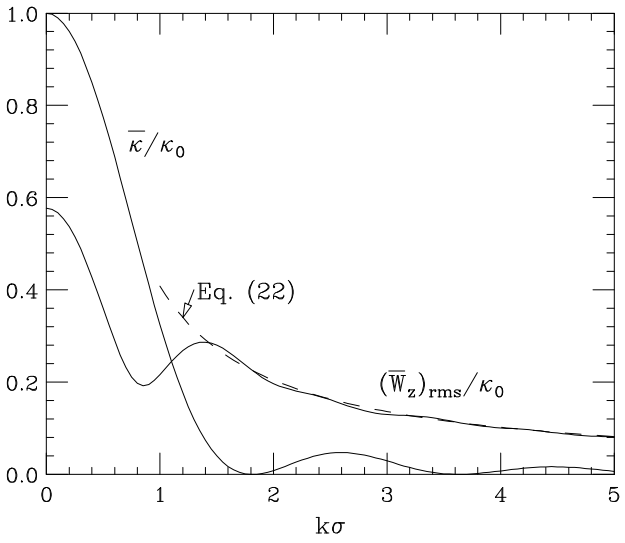

Figure 7: The interaction of a rectangular bunch of rms length σ and the resonator wakefield, with amplitude $2\varkappa_0$ and frequency k. Shown are the total bunch loss factor $\bar{\varkappa}$ and $(\bar{W}_z)_{rms}$ (the solid lines) and the asymptote, Eq. 22 (the dashes).

is simply given by

$$\bar{W}_z = -\frac{\varkappa_0}{\sqrt{3}k\sigma}\left(\sin ks + \sin\sqrt{3}k\sigma\right) \qquad [|s| \le \sqrt{3}\sigma] \quad . \tag{19}$$

The bunch loss factor becomes

$$\bar{\varkappa} = \varkappa_0 \left(\frac{\sin\sqrt{3}k\sigma}{\sqrt{3}k\sigma}\right)^2 \qquad , \tag{20}$$

and

$$(\bar{W}_z)_{rms} = \varkappa_0 \left[\frac{1}{6k^2\sigma^2}\left(1 - \frac{\sin 4\sqrt{3}k\sigma}{4\sqrt{3}k\sigma}\right) - \left(\frac{\sin\sqrt{3}k\sigma}{\sqrt{3}k\sigma}\right)^4\right]^{\frac{1}{2}} \quad . \tag{21}$$

For $k\sigma \gg 1$

$$(\bar{W}_z)_{rms} \approx \frac{\varkappa_0}{\sqrt{6}k\sigma} \qquad , \ [k\sigma \text{ large}]. \tag{22}$$

For the rectangular distribution the rms energy deviation drops at large k only as $(k\sigma)^{-1}$, and not as $(k\sigma)^{-2}$ as before. In Figs. 7 and 8 we have

repeated the calculations of Figs. 5 and 6 but for rectangular, rather than Gaussian, bunch distributions. In Fig. 7 note that both $\langle \bar{W}_z \rangle$ and $(\bar{W}_z)_{rms}$ are significant to larger values of $k\sigma$ than before. In Fig. 8 we note that, even for the long bunch case, the response is not inductive.

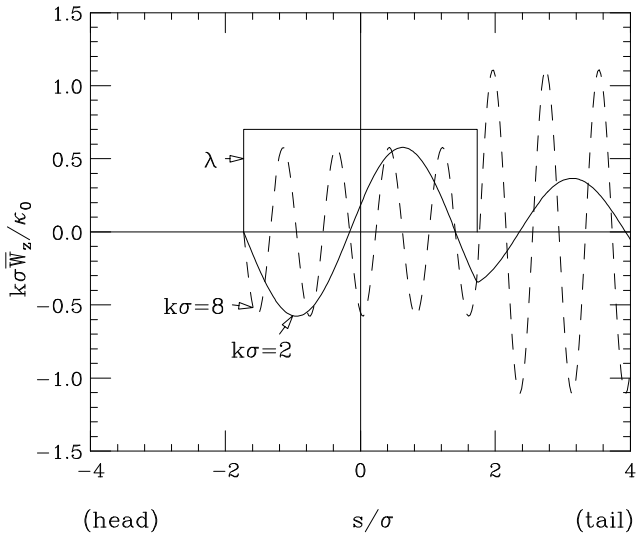

Figure 8: The bunch wake for a rectangular bunch in the presence of the resonator wakefield, when $k\sigma = 2$ and $k\sigma = 8$.

Application to the LCLS

According to the LCLS Design Report the most critical roughness impedance effect is expected to be the longitudinal effect in the undulator region. A change in average energy due to the roughness wake can be accommodated by tapering the undulator. Deviations from this average are limited to a window, outside of which particles will not lase throughout the undulator. In the LCLS Design report the tolerable limit is described either as an increase in rms energy spread of 0.05%, or as an energy window of $\pm 0.1\%$ about the mean.

The undulator length $L = 112$ m and the beam tube radius $a = 2.5$ mm; the bunch charge $eN = 1$ nC, the (useful) rms bunch length $\sigma \approx 15$ μm, and the beam energy $E = 14.3$ GeV. Let us begin by using the estimates of the inductive and resonator impedance models, Eq. 1 and Eqs. 3 and 6. For the inductive impedance model let us take $f = 2.$, $\alpha = 0.5$, and $\Delta = \delta/2$. We have obtained the average and rms energy deviation increase, $\langle \delta_E \rangle$ and

$(\delta_E)_{rms}$, and the fraction of beam within an energy window of $\pm 0.1\%$ from the mean, $n_{\pm .1\%}$; for both the inductive and resonator models; for Gaussian and rectangular bunch shapes with rms length $\sigma = 15$ μm; and for roughness sizes of $\delta = 1$, 0.1, and 0.01 μm. Note that these roughness sizes correspond to $k_{3d}\sigma = 1.0$, 3.2, and 10., respectively. Results are given in Table 1.

To meet the tolerance that $(\delta_E)_{rms} \leq 0.05\%$, for a Gaussian bunch shape, requires the roughness to be less than $\delta = 45$ nm for both the inductive and the resonator impedance models. The actual bunch shape is more rectangular than Gaussian. According to the resonator model, to meet the same tolerance for a rectangular bunch shape requires that the roughness be on the order of 3 nm. For the rectangular case, for the entire beam to be within a $\pm 0.1\%$ window requires that $\delta \approx 6$ nm. For such a bunch shape the inductive impedance model is not valid.

Table 1: The average and rms energy spread increase due to the roughness wakefields, and the fraction of beam within a window of $\pm 0.1\%$, at the end of the LCLS undulator, as given by the inductive and the resonator impedance models. Results are given for Gaussian and rectangular bunch shapes with rms length $\sigma = 15$ μm, and for roughness sizes $\delta = 1$, 0.1, 0.01 μm.

δ/μm	$k_{3d}\sigma$	Model	Bunch Shape	$\langle\delta_E\rangle/\%$	$(\delta_E)_{rms}/\%$	$n_{\pm .1\%}$
1.		Inductive	Gaussian	0	.79	.04
	1.0	Resonator	Gaussian	.83	.67	.04
			Rectangular	.73	.49	.06
.1		Inductive	Gaussian	0	.08	.69
	3.2	Resonator	Gaussian	.00	.10	.48
			Rectangular	.03	.29	.16
.01		Inductive	Gaussian	0	.01	1.
	10.	Resonator	Gaussian	.00	.01	1.
			Rectangular	.01	.09	.56

Instead of these idealized distributions let us apply the resonator model to a more realistic representation of the LCLS bunch shape. Taking the bunch shape given in the LCLS design report, and assuming a roughness size of $\delta = 50$ nm, we obtain the result given in Fig. 9. Shown are the current, I $(= eNc\lambda)$, and the resulting energy deviation δ_E. We see that most of the bunch is indeed rather rectangular, with a flat top ~ 3.4 kA. There is in addition, however, a rather pronounced tail including about 1/3

of the beam. Half of these tail particles have a large energy deviation and will not be useful. In following calculations, however, for simplicity, we will assume the entire tail is a loss, and not include any tail particles. The useful part of the beam has an rms length $\sigma = 13.2$ μm, and correspondingly $k_{3d}\sigma = 4.1$. According to the calculation $\langle\delta_E\rangle = 0.01\%$, $(\delta_E)_{rms} = 0.20\%$, and $n_{\pm.1\%} = 0.16$ (remember, 1/3rd of the loss is due to the tail). If $\delta = 10$ nm then these numbers become 0.00%, 0.07%, and 0.63, respectively.

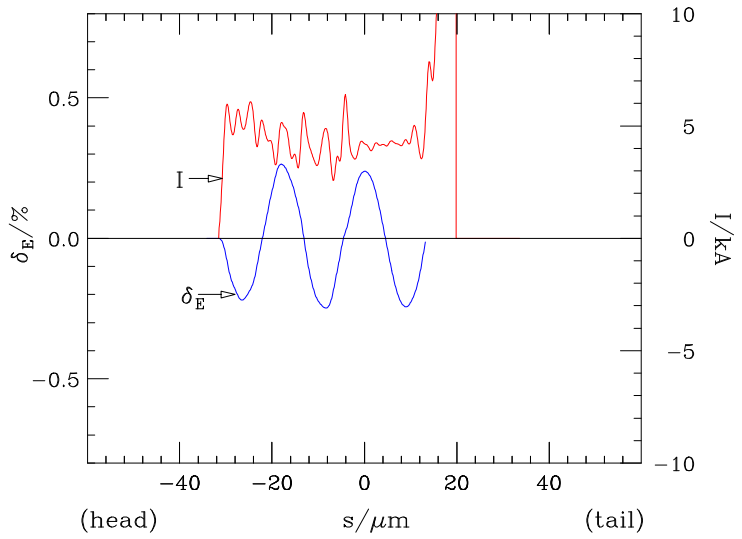

Figure 9: The bunch shape in the LCLS undulator (note $I = eNc\lambda$) and the resulting energy deviation (δ_E) predicted by the resonator impedance model, when $\delta = 50$ nm. Note that the 1/3rd of the beam is in the high current tail (not shown in its entirety).

Discussion

These results appear to set severe requirements on the beam tube surface smoothness. How smooth a beam tube surface can we expect to obtain? At present there is a program at SLAC to prepare and measure the inner surface of 2.5 mm radius beam tubes. Two preliminary observations suggest that the surface roughness effect may not be as severe as one might expect from the results above: (1) It appears that, through electro-polishing the surface, the effective depth δ can be reduced to 10–20 nm[21]. (2) The aspect ratio of roughness features, *i.e.* the period to depth of features, (p/δ), instead of being near 1 as assumed here, may be much larger, on the order of 50–

100[22]. According to calculations presented in Appendix B, for such aspect ratios the strength of the first resonance may be greatly suppressed. In fact, for the actual LCLS bunch shape, for $p/\delta = 50$ and a depth of $\delta = 100$ nm the results are still well within tolerances: $(\delta)_{rms} = 0.02\%$ and and the entire beam (outside of the tail particles) lies within $\delta_E = \pm 0.1\%$. An open question for this parameter regime, however, is how to account for the effect of the higher modes.

A Proposal to Measure the Roughness Wake at SLAC

To verify the models of roughness impedance it would be desirable to perform measurements. Since the effects are small, a beam tube with an artificially prepared surface, one with enhanced features, will probably be necessary. One program to measure the impedance of surface roughness is being planned for the Collimator Wakefield Test Facility to be constructed at SLAC[23]. It will employ two bunches, one to serve as driving bunch, the other as test bunch, to directly measure the effects of the transverse wakefields of an artificial "rough" surface. Here we suggest another measurement that can also be performed at SLAC, one which involves measuring the energy radiated by the beam due to the longitudinal roughness impedance. The idea is similar to that proposed for TESLA, and more details can be found in Ref. [24].

We propose that the inner surface of two cylindrically symmetric beam tubes be prepared and measured: one with a periodic array of shallow irises, the other with a surface of random bumps. Consider a normal SLAC linac bunch, which is Gaussian with rms length $\sigma = 0.5$ mm, and has a bunch population $N = 2 \times 10^{10}$. This bunch can excite frequencies up to 100 GHz. To match this to the frequency of the wall perturbation impedance we set the tube radius to $a = 1$ cm and the typical corrugation size to $\delta = 100$ μm (with $p \approx 2g$ and $p/\delta \lesssim 1$). The energy loss of the bunch is $U = e^2 N^2 \bar{\varkappa} L$, with L the tube length. For the tube with a periodic surface the pulse length of the radiation is given by $T = (1 - v_g/c)L/c$, with v_g the group velocity of the wave. The power generated is then (using Eqs. 8,9,10,17)

$$P = \frac{U}{T} \approx e^2 N^2 \frac{Z_0 c^2}{4\pi a \delta} e^{-4\sigma^2/a\delta} \quad . \tag{23}$$

For the parameters used here $v_g/c = 0.98$, $U \approx 0.7$ mJ (if L is 1 m), and $P \approx 10$ MW. For the random surface there will be some decoherence, and the power will be less.

Conclusion

We have compared the resonator impedance model of surface roughness to the inductive impedance model of roughness. We have shown that for long, smooth bunches the two models both give an inductive response, that the effective inductance per length is proportional to the corrugation depth over the beam pipe radius, and that the absolute results are also comparable. One can think of the inductive model as the asymptotic limit, for long bunches, of the resonator model. In the regime of long, smooth bunches, however, the inductive model may be more accurate, since the shape of the roughness features are also parameters in the model. (For example, for the version of inductive model of Ref. [5], the impedance is expressed in terms of the spectral function of the surface profile.)

For bunches that are not smooth, as is the case for the LCLS beam, the results of the two models diverge, and clearly the inductive impedance model no longer is valid (it predicts that the induced voltage is proportional to the derivative of the bunch shape). For a rectangular-shaped beam distribution, such as is found in the LCLS, the wakefield induced energy spread, according to the resonator model, decreases much more slowly as function of bunch length than it does for the equivalent Gaussian distribution. For the parameters in the LCLS undulator and with a roughness depth of 50 nm, this model predicts that the total induced rms energy spread becomes 0.17%, (which is larger than the allowable 0.05%), and 19% of the beam lies within an energy window of $\pm 0.1\%$. According to this model, for the entire bunch to be within tolerances requires a roughness depth of $\sim$ 10 nm.

It is not clear, at the moment, what the achievable surface smoothness for the undulator beam pipe can be, though preliminary measurements suggest that the effective perturbation depth may be kept to $\sim$ 10–20 nm, and the aspect ratio of the features—their period to depth ratio—may be very large $\sim$ 50–100. According to calculations, the strength of the resonance may be greatly suppressed in the case of a large aspect ratio. For an aspect ratio of 50 a roughness depth of 100 nm yields results for the fundamental mode that are still within tolerances. These results are preliminary, and much work still needs to be done before one can have confidence in their applicability. For example, to mention three outstanding problems: (1) how do we account for the effect of the higher modes for the case p/δ large; (2) it remains to be verified (possibly through time domain simulations) that for p/δ large, the periodic model can still be used to predict behavior for a random surface; and (3) a method—one that is valid also for the case of a non-smooth bunch shape—needs to be devised for obtaining the impedance

directly from roughness measurements of a beam tube surface.

Acknowledgments

The authors thank M. Cornacchia for inviting one of us (A.N.) to come for a short visit to SLAC to work on this problem, G. Stupakov and D. Walz for discussing preliminary results of their measurements of surface roughness, and P. Emma for supplying the LCLS bunch shape.

References

[1] A. Mosnier and A. Novokhatski, Proceedings of 1997 Part. Accel. Conf., Vancouver, Canada, p. 1661.

[2] K.L.F. Bane, C.K. Ng and A.W. Chao, Proceedings of 1997 Part. Accel. Conf., Vancouver, Canada, p. 1738, SLAC-PUB-7514 (1997).

[3] Linac Coherent Light Source (LCLS) Design Study Report, SLAC-R-521, April 1998.

[4] H.-D. Nuhn, "FEL Simulations for the LCLS," presented at FEL98, Williamsburg, VA, and SLAC-PUB-7912, August 1998.

[5] G. V. Stupakov, *Phys. Rev. ST-AB* **1**, 064401 (1998).

[6] K. Bane and G. V. Stupakov, "Wake of a Rough Beam Wall Surface," presented at ICAP98, Monterey, CA, and SLAC-PUB-8023, December 1998.

[7] K.-Y. Ng, *Phys. Rev. D* **42**, 1819 (1990).

[8] A. Burov and A. Novokhatski, Proceedings of XVth Intern. Linac Conf. on High Energy Accelerators, Hamburg, July 1992, p. 537.

[9] M. Dohlus, private communication.

[10] A. Novokhatski, M. Timm, T. Weiland, Proceedings of 1998 European Part. Accel. Conf., Stockholm, Sweden, p. 1350.

[11] A. Novokhatski, M. Timm, T. Weiland, "The Surface Roughness Wake Field Effect," presented at ICAP98, Monterrey, CA, Sept. 1998.

[12] R. Gluckstern, *Phys. Rev. D* **39**, 960 (1989).

[13] K. Bane, NLC Note 9, February 1995.

[14] A. Mosnier and A. Novokhatski, Proceedings of 1997 Part. Accel. Conf., Vancouver, Canada, p. 467.

[15] See, for example, K. Bane, M. Timm, T. Weiland, Proceedings of 1997 Part. Accel. Conf., Vancouver, Canada, p. 515 and DESY-M-97-02, January 1997.

[16] M. Chatard-Moulin and A. Papiernik, Proceedings of the 1979 Part. Accel. Conf., San Francisco, *IEEE Trans. Nucl. Sci.* **26**, 3523 (1979).

[17] R.K. Cooper, S. Krinsky, P.L. Morton, *Part. Accel.* **12**, 1-12 (1982); S. Krinsky, Proceedings of the 11^{th} Int. Conf. on High Energy Accelerators, CERN (Birkhäuser Verlag, Basel, 1980), p. 576.

[18] K. Bane and B. Zotter, Proceedings of the 11^{th} Int. Conf. on High Energy Accelerators, CERN (Birhäuser Verlag, Basel, 1980), p. 581.

[19] K. Bane and R. Ruth, in "Berkeley 1985, Proceedings, SSC Impedance," Berkeley, CA, 10 (1986); SLAC-PUB-3862, January 1986.

[20] P. Emma, private communication.

[21] D. Walz, private communication.

[22] R. Carr, G. Stupakov, D. Walz, report in preparation.

[23] P. Tenenbaum, for the Collimator Wakefield Facility study group.

[24] A. Novokhatski, "A Proposal for the Surface Roughness Wake Field Measurement in the TESLA Test Facility," TESLA–TTF Collaboration Meeting, Laboratori Nazionali di Frascati, November 1998.

Appendix A:
The Lowest Mode in a Beam Tube with Shallow Corrugations

The geometry of the corrugations is given in Fig. 2. We limit consideration here to the case δ/a small and p/δ not large. We follow the formalism of Ref. [18]: In the two regions, $r \leq a$ (the tube region, Region I) and $r \geq a$ (the cavity region, Region II) the Hertz vectors are expanded in a complete, orthogonal set; E_z and H_ϕ are matched at $r = a$; using orthogonality properties an infinite dimensional, homogeneous matrix equation is generated;

this matrix is truncated; and finally, the eigenfrequencies are found by setting its determinant to zero. We demonstrate below that, for our parameter regime, the system matrix can be reduced to dimension 1, and the results become quite simple.

In the tube region, let

$$\Pi_z^I = -\sum_{n=-\infty}^{\infty} \frac{A_n}{\chi_n^2} \frac{I_0(\chi_n r)}{I_0(\chi_n a)} e^{-j\beta_n z} \quad , \tag{A1}$$

with I_0 the modified Bessel function of the first kind, and

$$\beta_n = \beta_0 + \frac{2\pi n}{p} \quad , \quad \chi_n^2 = \beta_n^2 - k^2 \quad , \tag{A2}$$

with k the wave number of the mode. In the cavity region, let

$$\Pi_z^{II} = -\sum_{s=0}^{\infty} \frac{C_s}{\Gamma_s^2} \frac{R_0(\Gamma_s r)}{R_0(\Gamma_s a)} \cos[\alpha_s(z + g/2)] \quad , \tag{A3}$$

with

$$\alpha_s = \frac{\pi s}{g} \quad , \quad \Gamma_s^2 = \alpha_s^2 - k^2 \quad . \tag{A4}$$

R_0 is given by

$$R_0(\Gamma_s r) = K_0(\Gamma_s[a+\delta]) I_0(\Gamma_s r) - I_0(\Gamma_s[a+\delta]) K_0(\Gamma_s r) \quad , \tag{A5}$$

with K_0 the modified Bessel Function of the second kind.

E_z and H_ϕ are given by

$$E_z = \left(\frac{\partial^2}{\partial z^2} + k^2\right) \Pi_z \quad , \quad Z_0 H_\phi = -jk \frac{\partial \Pi_z}{\partial r} \quad , \tag{A6}$$

with $Z_0 = 120\pi\Omega$. Matching these fields at $r = a$, and using the orthogonality of $e^{-\beta_n z}$ on $[-p/2, p/2]$, and $\cos[\alpha_s(z + g/2)]$ on $[-g/2, g/2]$ we obtain a homogeneous matrix equation. To find the frequencies, the determinant is set to zero; *i.e.*

$$\det\left[\mathcal{R} - \left(\frac{2g}{p}\right) N^T \mathcal{I} N\right] = 0 \quad , \tag{A7}$$

with the matrix N given by

$$N_{ns} = \frac{2\beta_n}{(\beta_n^2 - \alpha_s^2)g} \begin{cases} \sin(\beta_n g/2) & : \ s \text{ even} \\ \cos(\beta_n g/2) & : \ s \text{ odd} \end{cases} \quad , \tag{A8}$$

and the diagonal matrices $\mathcal{R}$ and $\mathcal{I}$ by

$$\mathcal{R}_s = (1+\delta_{s0})ka\left(\frac{R_0'}{xR_0}\right)_{\Gamma_s a} \quad , \qquad \mathcal{I}_n = ka\left(\frac{I_0'}{xI_0}\right)_{\chi_n a} \quad . \tag{A9}$$

For the beam, on average, to interact with a mode, one space harmonic of the mode must be synchronous. We will pick the $n = 0$ space harmonic to be the synchronous one; *i.e.* let $\beta_0 = k$ (we take the particle velocity to be $v = c$). Let us truncate the system matrix to dimension 1, keeping only the $n = 0$ and $s = 0$ terms in the calculation. Now if $k\delta$ is small, then the $s = 0$ term in $\mathcal{R}$ becomes $\mathcal{R}_0 = 2/(k\delta)$, the $n = 0$ term in $\mathcal{I}$ is $\mathcal{I}_0 = ka/2$, and $N_{00} \approx 1$. Eq. A7 then yields

$$k = \sqrt{\frac{2p}{a\delta g}} \quad . \tag{A10}$$

As a check on consistency, note that for $s \neq 0$, $\Gamma_s a$ will be large (provided g/δ is not large), and $\mathcal{R}_s \sim \sqrt{g/a}$, which is small compared to the leading term. Similarly, for $n \neq 0$, $\chi_n a$ will be large (provided p/δ is not large), and $\mathcal{I}_n \sim \sqrt{p/a}$, which is small compared to the synchronous term.

The loss factor is given by $\varkappa = |V|^2/(4Up)$, where V is the voltage lost by the beam to the mode and U is the energy stored in the mode. The voltage lost in one cell is given by the synchronous ($n = 0$) space harmonic: $V = A_0 p$, and the energy stored in one cell, $U = 1/(2Z_0 c)\int E \cdot E^* \, dv$, is approximately that which is in the $n = 0$ space harmonic: $U = \pi A_0^2 a^2 p/(4Z_0 c)$ (for details, see Ref. [18]). The result is

$$\varkappa = \frac{Z_0 c}{2\pi a^2} \quad . \tag{A11}$$

To find the group velocity at the synchronous point, v_g, we take Eq. A7, truncate the matrices to dimension 1, and then expand near the synchronous point. Eq. A7 becomes

$$\frac{2}{k\delta} - \frac{gka}{p}\left[1 - \frac{(\beta_0^2 - k^2)a^2}{8}\right] = 0 \quad . \tag{A12}$$

Taking the derivative with respect to β_0 ($dk/d\beta_0 = v_g/c$), and then setting $\beta_0 = k$ we obtain the result:

$$(1 - v_g/c) \approx \frac{8}{k^2 a^2} = \frac{4\delta g}{ap} \quad . \tag{A13}$$

The above method can be extended to modes of higher multipole moment m, in which case the beam will excite hybrid modes rather than the pure TM modes of above[18]. Again the system matrix can be reduced to the $n = 0$ and $s = 0$ terms, and the lowest mode wave number has a simple form:

$$k = \sqrt{\frac{(m+1)p}{a\delta g}} \qquad , \qquad [1 \leq m \ll a/\delta] \quad . \tag{A14}$$

In particular, we note that the dipole mode ($m = 1$) frequency is equal to the monopole ($m = 0$) frequency.

Note that all the above formulas are not valid when p/δ is sufficiently large, a case studied in Appendix B.

Appendix B: Suppression of the Lowest Mode when p/δ is Large

To study the sensitivity of the impedance on the aspect ratio p/δ we have performed more TRANSVRS simulations. For larger p/δ, to obtain accurate results, the system matrix must be kept sufficiently large; it cannot be truncated to dimension 1. The results are summarized in Fig. 10, with frame (a) giving the frequency and frame (b) the loss factor of the lowest mode. The curve in frame (a) gives the location of the 2nd mode frequency $k = \pi/p$. The frequency is normalized to the analytic approximation k_0, given in Eq. 8, and the loss factor to $\varkappa_0$, given in Eq. 9. We expect the loss factor to become very small by the time the period reaches $p_0 = \pi/k_0$, *i.e.* by

$$p_0 = \pi\sqrt{\frac{a\delta g}{2p}} \qquad , \tag{B1}$$

and we normalize the abscissa to this parameter.

We see in Fig. 10 that for p/δ small we obtain the analytical results, $k = k_0$ and $\varkappa = \varkappa_0$, but as p/δ increases, k begins to increase and $\varkappa$ decreases. Eventually the frequency of the lowest mode also follows the curve $k = \pi/p$. In the four examples in the figure, by the time $p \approx p_0$ the loss factor of the first mode has become very small. At $\delta/a = 0.001$, for example, $p = p_0$ corresponds to $p/\delta \approx 50$. In Table 2 we give an example calculation for the LCLS undulator parameters, for the case $\delta = 100$ nm and $p/\delta = 50$, and for a rectangularly shaped bunch with $\sigma = 15$ μm. Note that the tolerance on $(\delta_E)_{rms}$ is met, and that the entire beam is within the energy window of $\pm 0.1\%$; this is quite different than was found in Table 1 for the case $\delta = 100$ nm and $p \approx \delta$. Repeating the calculation for the same

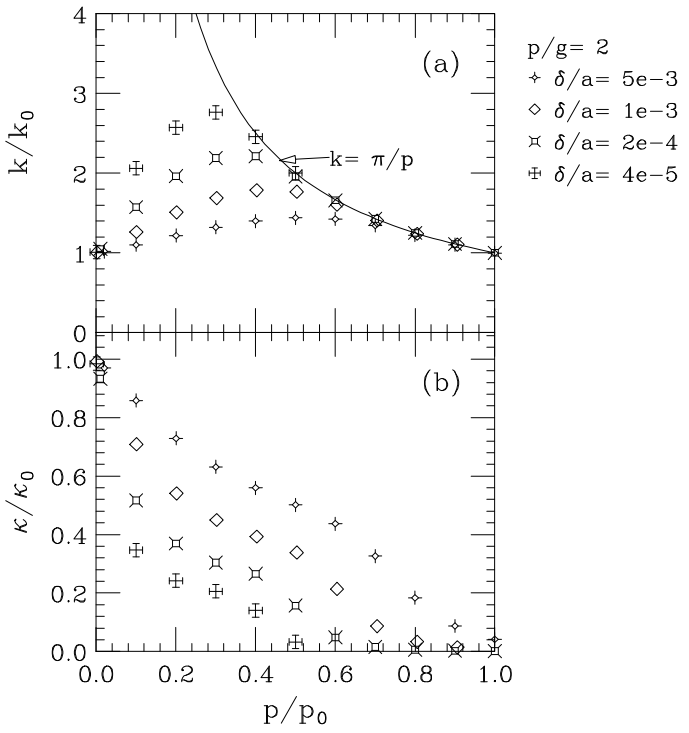

Figure 10: Dependence of the (lowest) synchronous mode frequency (a) and corresponding loss factor (b) of a corrugated tube on the aspect ratio of the corrugations, as obtained by TRANSVRS (the plotting symbols). The period $p = 2g$. Results are given for several values of δ/a. The results are normalized to $p_0 = \pi\sqrt{a\delta g/2p}$, $k_0 = \sqrt{2p/a\delta g}$, and $\varkappa_0 = Z_0 c/(2\pi a^2)$.

geometry and the actual LCLS bunch shape, we obtain $(\delta_E)_{rms} = .02\%$ and $n_{\pm.1\%} = 0.7$.

The Effect of the Higher Modes

When the fundamental mode is partially suppressed part of its impedance (loss factor) is spread over many, higher frequency modes, since for *any* periodic structure the sum of the loss factors of all modes must equal $Z_0 c/(2\pi a^2)$. In this case what is left are many weak, closely spaced modes beginning at frequencies just beyond $k = \pi/p$. Since the modes are at higher frequencies, their interaction with a beam becomes weaker: we have seen that the bunch loss decreases as $(k\sigma)^{-2}$ and $(k\sigma)^{-1}$ for, respectively, a Gaussian and a rectangular bunch, at high frequencies (see Eqs. 18,22). As an upper limit of

Table 2: An example of suppression of the dominant mode of the roughness wakefield when the aspect ratio p/δ of the wall undulation becomes large. Given are the increase in rms energy spread at the end of the LCLS undulator and the fraction of beam within a window of $\pm 0.1\%$ for the case $\delta = 100$ nm and $p/\delta = 50$. The bunch shape is rectangular with rms length $\sigma = 15$ μm.

δ/μm	p/μm	p/p_0	k/k_0	$k_{3d}\sigma$	$\varkappa/\varkappa_0$	$(\delta_E)_{rms}/\%$	$n_{\pm.1\%}$
.1	5.	.20	2.65	8.70	.25	.025	1.0

the wakefield interaction, we can take the residual impedance (loss factor), *i.e.* that portion that is not in the fundamental, to be in the second mode at frequency $k = \pi/p$. For example, for the rectangular bunch, the LCLS parameters, and the roughness geometry of Table 2, the fundamental mode loss factor $\varkappa = 0.25\varkappa_0$. This upper limit of wakefield interaction is found by taking the second mode to have loss factor $\varkappa = 0.75\varkappa_0$ and frequency $k = \pi/p$. For the second mode $k\sigma = 9.4$, and this limit says that the contribution to the induced rms energy variation of the higher modes (using Eqs. 12,22) is $\leq 0.09\%$, which is still larger than the specified tolerance. Note that for $p \gtrsim p_0$ this limit predicts that the interaction can be stronger than for the (unsuppressed) single, resonator impedance.

For a more detailed understanding of the higher mode impedances, at least for the specific case of a wall with smooth undulations, one can refer to the perturbation theory of Chatard-Moulin and Papiernik[16]. Their theory is valid so long as the depth of undulation over the beam pipe radius is small, and the slope of the wall perturbations is everywhere small. Their analytic result gives an infinite series of weak, closely spaced modes connected to every Fourier harmonic of the wall undulations. Their result is valid only if, for all harmonics, the period to amplitude ratio is sufficiently large, and therefore, is not valid for the type of rectangular geometry used in TRANSVRS (shown in Fig. 2). If the wall shape is written in the form $a[1 + \sum C_q \exp(2\pi i q' z/p)]$, with q' going from $-\infty$ to ∞ but with no $q' = 0$ term, then the wave number and loss factor of mode (q, s) [with $q = |q'|$] are given by

$$k_{qs} = \frac{\pi q}{p}\left[1 + \left(\frac{j_{0s}p}{2\pi qa}\right)^2\right] \quad , \tag{B2}$$

$$\varkappa_{qs} = \frac{\pi Z_0 c}{p^2} q^2 |C_q|^2 \left[1 + \left(\frac{j_{0s}p}{2\pi qa}\right)^2\right] \quad , \tag{B3}$$

with j_{0s} the s^{th} zero of the Bessel function J_0. Note that there must be some s limitation to the validity of Eq. B3, since summing the loss factors over s gives a divergent solution, and the sum should equal $Z_0 c/2\pi a^2$. It, therefore, is not clear how one can use the results of the Chatard-Moulin and Papiernik to obtain the total impedance, even for the case of a wall with smooth undulations.

Finally, even though the perturbation method is not in principle applicable to the rectangular geometry solved for in TRANSVRS, from curiosity we have performed one comparison run for the case period over depth, p/δ, large. For our example we take $\delta/a = 1 \times 10^{-3}$, $p/g = 2$, $p/a = 0.05$, and therefore, $p/\delta = 50$ and $p/p_0 = 1$. The results for the first 16 modes are shown in Fig. 11 (the plotting symbols). For comparison we take the perturbation solution, keeping the lowest Fourier harmonic, for which $C_1 = -i\delta/(\pi a)$ and $C_{-1} = -C_1$ (these results are given by the curves in Fig. 11). We note that the computed frequencies are nearly identical to those of the perturbation method. As for the loss factors, the first is much larger than the analytical one (it has not yet been fully suppressed) while the others are all about a factor of 2 larger. These preliminary results are suggestive, and this parameter regime will be the subject of a future study.

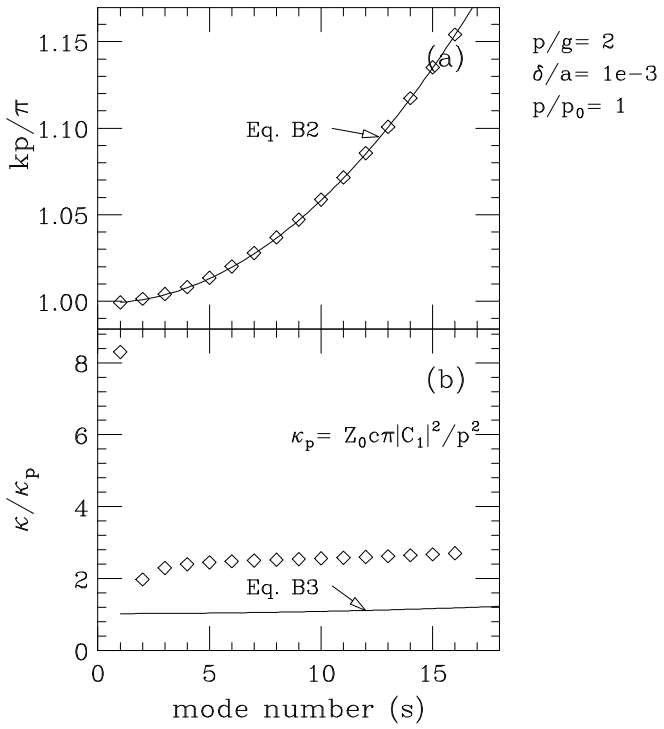

Figure 11: The first 16 computed frequencies (a) and loss factors (b) for a case with p/δ large. The parameters are $\delta/a = 1\times10^{-3}$, $p/g = 2$, $p/a = 0.05$, and therefore, $p/\delta = 50$ and $p/p_0 = 1$. The curves give the perturbation result of Chatard-Moulin and Papiernik, with $C_1 = -i\delta/(\pi a)$ and $C_{-1} = -C_1$, the first Fourier harmonics of the boundary geometry.